# Sulphonated mesoporous silica-carbon composites and their use as solid acid catalysts

Patricia Valle-Vigón, Marta Sevilla and Antonio B. Fuertes*

Instituto Nacional del Carbón (CSIC), P. O. Box 73, 33080-Oviedo, Spain

* Corresponding author (**E-mail:** abefu@incar.csic.es**)**

**Abstract**

The synthesis of highly functionalized porous silica-carbon composites made up of sulphonic groups attached to a carbon layer coating the pores of three types of mesostructured silica (*i.e.* SBA-15, KIT-6 and mesocellular silica) is presented. The synthesis procedure involves the following steps: a) removal of the surfactant, b) impregnation of the silica pores with a carbon precursor, c) carbonization and d) sulphonation. The resulting silica-carbon composites contain ~ 30 wt % of carbonaceous matter with a high density of acidic groups attached to the deposited carbon (*i.e.* -$SO_3H$, -COOH and -OH). The structural characteristics of the parent silica are retained in the composite materials, which exhibit a high surface area, a large pore volume and a well-ordered porosity made up uniform mesopores. The high density of the sulphonic groups in combination with the mesoporous structure of the composites ensure that a large number of active sites are easily accessible to reactants. These sulphonated silica-carbon composites behave as eco-friendly, active, selective, water tolerant and recyclable solid acids. In this study we demonstrate the usefulness of these composites as solid acid catalysts for the esterification of maleic anhydride, succinic acid and oleic acid with ethanol. These composites exhibit a superior intrinsic catalytic activity to other commercial solid acids such as Amberlyst-15.

## 1. Introduction

Inorganic acids (*i.e.* $H_2SO_4$, HF and $H_3PO_4$), are commonly employed as homogeneous catalysts for the synthesis of important industrial and pharmaceutical chemical products such as alcohols, esters, ethers and starting materials of polymers or resins, and, more recently, for the production of biodiesel [1]. However, these catalysts present several drawbacks. They can cause serious environmental and corrosion problems, they are costly and the processes for separating them from the products are ineffective. Furthermore, the waste streams need to be neutralized. This explains why the search for green, recyclable, easily separable and highly active catalysts to replace the traditional homogeneous ones has occupied a prominent place in recent research [2-5]. Numerous heterogeneous solid acids have been developed [6], including inorganic-oxide solids such as zeolites and niobic acid [5,7], strong acidic ion exchange resins (*i.e.* Amberlyst or Nafion) [8,9], sulphonated zirconia [10] and carbon-based materials [11-13]. The discovery of mesostructured silica materials has made it possible to design a new type of solid acid by grafting $SO_3H$ groups to the surface of the silica pores [14]. These catalysts have a large surface area and pore volume in combination with tunable and large pore sizes, which makes the active sites easily accessible [15,16]. However, the synthesis procedure for fabricating these catalysts is complex and involves multiple steps, at the end of which only relative low -$SO_3H$ densities are achieved [17].

Sulphonated ordered mesoporous carbons (OMCs), synthesized by the nanocasting technique [18,19], have recently emerged as promising acid catalysts due to the fact that they can be easily functionalized with a large number of acid groups [18-22]. However, the complex and time consuming synthesis procedures considerable limit their applicability. As an alternative, mesoporous silica-carbon composites have emerged as a new class of promising solid acid catalysts. Because of their unique

characteristics it is possible to combine the structural properties typical of mesoporous silica, *i.e.* a high surface area and uniform porosity, with the easy functionalization of carbon materials. Moreover, it has been demonstrated that these composites have a much better hydrothermal and mechanical stability than carbonaceous materials [23]. Several procedures for coating the silica pores with a carbon layer have been previously reported. Zhang et al. described a procedure for depositing carbon inside the silica pores by means of a CVD process [24]. Nishihara et al. synthesized carbon-coated SBA-15 by attaching 2,3-dihydroxynaphthalene to the silica pores followed by a carbonization step [25]. Recently, we presented a novel route for fabricating silica-carbon composites in which the carbon layer coating the silica pores is produced by the carbonization of the surfactant used as the structure-directing agent to synthesize mesostructured silica [26]. Sulphonation of the carbon layer deposited inside the silica pores is a simple way to fabricate well-structured solid acid catalysts with easily accessible pores [27]. This alternative, however, has only been explored by a few authors. Thus, Nakajima et al. [28] and Fang et al. [29] reported a method for preparing sulphonated silica-carbon composites in which the carbon layer was produced by the impregnation, polymerization and carbonization of a mixture of glucose and $H_2SO_4$ inside the pores of SBA-15 silica. However, these authors failed to obtain a uniform carbon layer when > 20 % of carbon was deposited. The reason for this was that carbon was plugging the mesopore channels, resulting in a microporous material and a decrease in catalytic activity as confirmed by the dimerization of α-methylstyrene. Likewise, Liu et al. described the synthesis of sulphonated silica-carbon composites using sucrose as carbon precursor and MCM-48 as silica substrate [30]. These materials were used to esterify acetic acid with n-butyl alcohol. They were also employed for esterifying caprylic acid, lauric acid and hexadecanoic acid with ethanol.

In the present work, we propose a novel method for producing sulphonated mesoporous silica-carbon composites made up of a thin layer of carbon with a high density of -$SO_3H$ groups covering the internal surface of the pores of three types of mesoporous silica. The method involves a mild surfactant removal procedure which allows the preservation of a high concentration of silanol groups inside the internal surface of the silica substrates. These silanol groups act as anchoring sites for the carbon precursor molecules (*i.e.* 2,3-dihydroxynaphthalene) giving rise to a homogeneous layer of carbon coating the silica pores. Subsequent treatment of the silica-carbon samples with sulphuric acid produces sulphonated composites with a high concentration of -$SO_3H$ groups uniformly distributed along the porosity. We further prove their successful application as solid acid catalysts in the esterification of several organic acids (*i.e.* maleic anhydride, succinic acid and oleic acid) with ethanol.

## 2. Experimental

### *2.1. Synthesis of the silica-carbon composites*

Three types of mesostructured silica materials (*i.e.* SBA-15, KIT-6 and mesocellular silica) were employed for the preparation of the composites. The SBA-15 silica was synthesized according to the procedure reported by Zhao et al [31], whereas KIT-6 mesostructured silica and mesocellular silica (MS) were prepared as described by Kleitz et al [32] and Stucky et al [33] respectively. In order to remove the surfactant, the as-synthesized hybrid silica-surfactant materials were solvent-extracted using a mixture of 4 mL of HCl (37 wt %) and 200 mL of ethanol per gram of sample. This procedure was performed twice at 80 °C (reflux), and after each extraction, the silica was filtered, washed with ethanol and water, and dried [34].

The preparation of the silica-carbon composites was carried out according to the procedure reported by Nishihara et al. using 2,3- dihydroxynaphthalene (DN) as carbon precursor [25]. In a typical synthesis, 1.5 g of silica was added to a solution of 3 g of DN in 75 mL of acetone and the mixture was stirred for several hours at room temperature in a closed vessel. Then, the acetone was allowed to evaporate at room temperature overnight and the sample was dried at 80 ºC. The solid mixture was heat-treated at 300 ºC for 1 h under a $N_2$ flow. The unreacted DN was removed by washing with acetone and the DN-silica composite was heat-treated under vacuum at temperatures in the 450-550 ºC range for 2 h. The silica-carbon composites thus obtained were denoted as C*X*-*Y*, where *X* = S, K or MS for SBA-15, KIT-6 and mesocellular silica respectively, and *Y* is the heat-treatment temperature.

*2.2. Sulphonation of silica-carbon composites*

Sulphonation was carried out by mixing 1 gram of silica-carbon composite with 25 mL of concentrated sulphuric acid (98%, Prolabo) in a 50 mL round-bottomed flask. The mixture was heated for 15 h at 150 ºC under $N_2$. The solid was then washed (Soxhlet extraction) with distilled water until the washing water was completely free of sulphate ions. The resulting sulphonated silica-carbon composites were denoted as CS*X*-*Y*.

*2.3. Characterisation of the materials*

Small and wide angle X-ray diffraction (XRD) patterns were obtained on a Siemens D5000 instrument operating at 40 kV and 20 mA, using CuK*a* radiation ($\lambda$=0.15406 nm). Scanning and Transmission Electron images (SEM and TEM) were taken on a Zeiss DSM 942 microscope and on a JEOL (JEM-2000 EX II) microscope operating at 160 kV respectively. Nitrogen sorption isotherms were performed at -196ºC

on a Micromeritics ASAP 2020 volumetric adsorption system. The BET surface area was deduced from the analysis of the isotherms in the relative pressure range of 0.04-0.20. The volume was calculated from the amount adsorbed at a relative pressure of 0.99. The pore size distributions (PSDs) were determined by applying the Kruk-Jaroniec–Sayari (KJS) method to the adsorption branch [35]. Diffuse reflectance Fourier-Transform Infrared (FT-IR) spectra of the materials were recorded on a Nicolet Magna-IR 560 spectrometer fitted with a diffuse reflection attachment. The carbonaceous matter content in the composites was deduced by thermogravimetric analysis on a CI Electronics system. X-ray photoelectron spectroscopy (XPS) was carried out on a Specs spectrometer, using MgKα (1253.6 eV) radiation from a double anode at 50 w. Binding energies for the high-resolution spectra were calibrated by setting C 1s to 284.6 eV. Temperature programmed desorption (TPD) experiments were performed in a chemisorption analyzer (Micromeritics, Autochem II) equipped with a mass spectrometer (OmniStar 300O). The Raman spectra were recorded on a Horiva (LabRam HR-800) spectrometer. The sulphonic acid density was estimated from the total sulphur content of each sample, as determined by elemental analysis on a LECO S-144DR analyzer. Acid densities were estimated by neutralization titration. The total content of acidic groups (i.e. -$SO_3H$, -COOH and -OH) and the content of the strongest acidic groups (i.e. -COOH and -$SO_3H$ groups) were estimated by titration with NaOH (0.05 N) and $NaHCO_3$ (0.05 N), respectively. Then, carboxylic and hydroxyl densities were calculated from the combination of the titration results and the elemental sulphur content.

*2.4. Catalytic activity of the sulphonated silica-carbon composites*

The sulphonated mesoporous silica-carbon composites were employed as solid acids for the esterification of maleic anhydride, succinic acid and oleic acid with

ethanol. In all the cases, Amberlyst 15 was taken as the reference catalyst, and ethanol was used in molar excess to steer the equilibrium towards the formation of ester. Prior to the reaction, all the catalysts were dried at 120 ºC for 3 h, except for Amberlyst-15 which was vacuum dried at 110 ºC for 4 h. The experiments were carried out by mixing the reactant and ethanol (see specific amounts in Table S1) in a 25 mL round-bottomed flask equipped with a reflux condenser and a magnetic stirrer. Once the mixture had reached the reflux temperature, the catalyst was added. Aliquots were periodically withdrawn and centrifuged to separate the solution from the catalyst. Analysis of the reaction mixtures was carried out in a HP 6890 series gas chromatograph equipped with a flame ionization detector (FID) and a HP-5 capillary column (30m x 0.25 mm x 0.25 μm).

Recycling experiments were performed to determine the operational stability of the prepared catalysts. At the end of each esterification cycle, the catalyst was centrifuged, washed with acetone and dried before reuse.

## 3. Results and Discussion

Mesoporous silica-carbon composites were prepared using three types of mesostructured silica, *i.e.* SBA-15, KIT-6 and mesocellular silica. 2,3-dihydroxynaphthalene (DN) was chosen as carbon precursor because a) its aromatic structure favours the formation of carbonaceous matter without specific heteroatoms and b) it has been reported as good precursor to obtain a thin carbon layer coating the silica pores [25]. The synthesis procedure for preparing sulphonated mesoporous silica-carbon composites is illustrated in Scheme 1. In a first step, the surfactant employed in the synthesis of silica was removed by means of a mild procedure (*i.e.* solvent extraction).The resulting silica was then impregnated with the carbon precursor

(*i.e.* 2,3-dihydroxynaphthalene) which reacts with the silanol groups via a condensation reaction. This ensures uniform distribution of the carbon precursor inside the silica pores. Subsequently, the impregnated silica was heat treated at temperatures in the 450-550 ºC range. In this way, DN was converted into a carbonaceous material coating the silica pores. Finally, the silica-carbon composite was treated with concentrated sulphuric acid, giving rise to the formation of sulphonic groups attached to the carbon layer.

*3.1. Structural characteristics of the silica-carbon composites*

As shown in Scheme 1, the silica-DN hybrid material is generated from the impregnated silica through condensation reactions between the silanol groups on the pore surface of the silica and the hydroxyl groups in DN [25]. Therefore, in order to maximize the amount of carbonaceous matter deposited within the silica pores, it is important to preserve a large number of surface silanol groups. In this work, to maintain a high concentration of silanol groups, the surfactant was removed by means of a solvent-extraction procedure instead of by calcination [34]. The silica-carbon composites produced in this way contain around 30 wt % of carbonaceous matter (see Table 1). This amount is much greater than that obtained when the surfactant is eliminated by means of air calcination (< 20 wt %). This proves that the use of silica substrates with a large density of silanol groups is crucial to maximizing the amount of deposited carbon.

Figure 1 shows the electron microphotographs of SBA-15, KIT-6 and MS silica samples and their corresponding silica-carbon composites. For all the silica-carbon composites, it can be seen that, despite the large amount of deposited carbon, they retain the morphology of the parent silica, there being no appreciable amounts of carbon

deposits on the outer surface of the particles (Figure 1). Interestingly, in the case of mesocellular silica it can be observed that the large mesopores are empty (Figures 1G and 1H). These results suggest that the carbon layer is exclusively located inside the silica pores.

The incorporation of carbonaceous matter into the silica pores leads to a moderate reduction in the textural properties of the composites (BET surface area, pore volume and pore size) with respect to the parent silicas (Table 1). The $N_2$ sorption isotherms (Figure 2), show a pronounced capillary condensation step at $p/p_0 \sim 0.6 – 0.8$, indicating the presence of well-developed and uniform mesopores. This is confirmed by the pore size distributions in Figure 2 (insets). These mesopores have a size in the 8-11 nm range in the case of SBA-15, KIT-6-based materials and ~ 28 nm in the case of the samples obtained from mesocellular silica. The thickness of the deposited carbon layer can be deduced from the difference between the mean pore size of silica and the silica-carbon composite. Thus, for the SBA-15, KIT-6/carbon composites, a carbon thickness of ~ 0.7 nm was recorded, which is equivalent to the thickness of two graphene sheets. Low angle-range XRD patterns of the SBA-15, KIT-6/carbon composites reveal that the structural order is maintained after carbonization (see Figure S1). This result is also confirmed by the TEM images of the SBA-15, KIT-6 and MS/carbon composites (Figure 3A, 3C and 3E respectively). These findings suggest a uniform distribution of the carbon deposited inside the pores of the silica. To obtain more information about the distribution of the carbon deposited inside the silica-carbon composites, we examined the structure of a templated carbon obtained by dissolving the silica skeleton of a SBA-15/carbon composite. SEM inspection revealed that the templated carbon particles are made up of a bundle of nanorods (Figure S2a). The templated carbon C(S) has a large BET surface area (1080 $m^{2}{\cdot}g^{-1}$) and a high porosity predominantly made up of

mesopores of uniform size centered at ~ 3.9 nm (see Figure S2b and Table 1). These data suggest that the carbon deposited inside the pores of the silica-carbon composites forms an interconnected structure uniformly distributed inside the porosity of the silica.

*3.2 Sulphonated silica-carbon materials*

In order to produce solid acid catalysts, the prepared silica-carbon composites were sulphonated following the synthesis procedure illustrated in Scheme 1. The SEM images in Figure 1 (C, F and I) indicate that sulphonation does not entail any change in the morphology or particle size of the sulphonated composites. What is more, comparison of the low angle-range XRD patterns (Figure S1) and TEM images (Figure 3) obtained for the parent silica materials and the corresponding sulphonated composites, reveals that the pore structure is hardly affected at all by the carbonization-sulphonation steps. This is further supported by the analysis of the $N_2$ sorption isotherms in Figure 2 and Figure S3. Only a slight modification of the textural parameters is observed for the carbonized or sulphonated samples in relation to the parent silica (see Table 1). It is worth noting that an increase in the values of surface area, pore volume and pore size is observed for the sulphonated samples with respect to non-sulphonated silica-carbon composites. This may be due to the fact that during the sulphonation stage, in parallel with the introduction of sulphonic groups, oxidation and dehydration reactions in the carbonaceous matter take place, leading to a partial gasification of the deposited carbon and an enhancement of the porosity [18,36]. This is confirmed by thermogravimetric analysis (data not shown), which reveals that the sulphonation process produces a loss in carbonaceous matter of ~ 5 wt %. It should be mentioned that, whereas the sulphonation of templated carbons causes the total destruction of their pore structure [37] or pore ordering [21], in the case of the silica-carbon composites the mesostructure is retained even after sulphonation. This is due to

the fact that the silica framework acts as a support for the carbon layer, thereby avoiding its collapse [18,21,37].

*3.3. Chemical properties of the sulphonated silica-carbon composites*

Several works have shown that carbonization temperatures higher than 600 ºC lead to well-structured carbons but ones which are highly resistant to functionalization. In contrast, moderate carbonization temperatures give rise to a partially carbonized material which contains a large number of chemically reactive carbon sheets lacking in structural rigidity [18,38]. Silica-carbon composites can combine both characteristics, a structurally sound silica framework which preserves the mesoporous structure and makes the pores easily accessible to the reactants. At the same time a partially carbonized carbon layer would provide reactive aromatic carbon sheets that facilitate the attachment of $-SO_3H$ groups. To this end, sulphonation was carried out on silica-carbon composites carbonized at moderate temperatures (*i.e.* 450, 500 and 550 ºC). From the results listed in Table S2 it can be seen that the carbonization temperature in the 450-550 ºC range hardly affects the textural properties or content of the $-SO_3H$ groups in the sulphonated composites.

The chemical nature of the functionalized carbon deposited inside the silica pores was investigated by infrared, X-ray photoelectron and Raman spectroscopic techniques. A comparison of the FT-IR spectra for the silica (SBA-15), CS-500 silica-carbon composite and for sulphonated silica-carbon samples is presented in Figure 4. The SBA-15 silica exhibits two characteristic FT-IR bands at 1000-1300 $cm^{-1}$ and ~ 800 $cm^{-1}$ corresponding to asymmetric and symmetric stretching vibrations of the Si-O–Si and a broad band at 2600-3800 $cm^{-1}$ caused by the O-H stretching of H bonded O-H [39-41]. After the incorporation of carbon (*i.e.* the CS-500 sample), the

characteristic FT-IR band associated to the OH stretching vibrations from silanol groups (2600-3800 $cm^{-1}$) completely disappears. This suggests that the carbon layer uniformly coats the silica pores. Moreover, this sample exhibits several new peaks corresponding to C=C stretching vibrations at 1630 $cm^{-1}$ and C–H out-of-plane deformation vibrations at 750 $cm^{-1}$ [25]. In the case of the sulphonated samples (*i.e.* CSS-500, CSK-500 and CSMS-500), a new band appears at 1050-1080 $cm^{-1}$ corresponding to a S=O symmetric stretching vibration, indicating that sulphonic groups are attached to the carbon surface [26]. The IR spectra of the sulphonated samples also show other bands assigned to O-H stretching (3200-3700 $cm^{-1}$) and C=O stretching (1740 $cm^{-1}$) vibrations, together with an increase in intensity of the C=C stretching vibration band (~1640 $cm^{-1}$). The generation of these O-groups occurs because, in parallel with the insertion of -$SO_3H$ groups, oxidation reactions within the carboneous layer are taking place as a consequence of the action of sulphuric acid.

The nature of the sulphur functionalities present in the silica-carbon composites was further investigated by XPS. Figure 5a shows the S 2p core-level spectrum for a sulphonated KIT-6/carbon sample (CSK-500). It contains one single doublet at around 168 eV which is associated to -$SO_3H$ groups [38,42]. The presence of sulphonic groups was also confirmed by Raman spectroscopy. The spectra shown in Figure 5b exhibit, in addition to the typical D and G-mode bands associated to benzene rings of amorphous carbon (1350 $cm^{-1}$) and graphene sheets (1580 $cm^{-1}$) [26,43], a band at 1150 $cm^{-1}$ that may be attributed to sulphonic groups [44].

In order to analyze the thermal stability of the sulphonic groups attached to the carbon layer, temperature programmed desorption (TPD) experiments were carried out. Figure 6 shows the TPD profiles for $SO_2$, CO and $CO_2$ obtained by thermal treatment of the sulphonated silica-carbon CSS-500 composite under an inert atmosphere. It can be

seen that $SO_2$ evolution as a consequence of the decomposition of -$SO_3H$ groups occurs in the 150 - 650 ºC temperature range. This result shows that a temperature of 150 ºC is the maximum temperature at which this material can be used as a solid acid catalyst. A large amount of CO and $CO_2$ is released in the same range of temperatures as that of $SO_2$ (see Figure 6). This occurs because of the decomposition of the -$SO_3H$ groups, giving rise to the formation of $SO_3$ that acts as an oxidant of the carbon according to the reaction: $SO_3 + C \rightarrow SO_2 + CO/CO_2$ [36,42]. Similarly, more CO and $CO_2$ may be generated at high temperatures as a result of the decomposition of the different oxygen acid groups (*i.e.* carboxylic acids, carboxylic anhydrides and phenols) produced during the sulphonation stage.

The acid functional groups (*i.e.* -$SO_3H$, -OH and -COOH) present in the sulphonated samples were quantified by elemental analysis (S content) and titration. The results, listed in Table 2, reveal that the sulphonated composites have a high acid density (2.5-4 $mmol \cdot g^{-1}$). Strong acid groups associated to -$SO_3H$ functionalities represent ~ 10 % of total acidity (0.25-0.4 $mmol \cdot g^{-1}$). The rest corresponds to carboxylic (0.85-1.2 $mmol \cdot g^{-1}$) and hydroxyl (1.6-2.4 $mmol \cdot g^{-1}$) groups. Interestingly, the concentration of -$SO_3H$ groups attached to the composites is greater than that reported by other authors for other types of sulphonated silica-carbon composites [28].

*3.3. Catalytic activity of the sulphonated silica-carbon composites*

Bearing in mind the structural and chemical properties of sulphonated silica-carbon composites, we analyzed their use as solid acid catalysts in several esterification reactions of practical interest. The esterification reactions of maleic anhydride, succinic acid and oleic acid with ethanol were selected to examine the catalytic performance of these composites The schemes of these esterification reactions are shown in Figure 7

together with the profiles corresponding to the formation of diethyl maleate (DEM, Figure 7a), diethyl succinate (DIES, Figure 7b) and ethyl oleate (OE, Figure 7c). The catalytic performance of Amberlyst-15, which is used as reference, is also included in these figures. The values of the initial reaction rate, selectivity (S) and turnover frequency (TOF) are listed in Table 3. The results (Figure 7) reveal that the use of sulphonated composites gives rise to high product yields (*i.e.* 40-60 % DEM, 100 % DIES and 70-80 % OE), comparable to those obtained with a commercial solid acid such as Amberlyst-15. The initial reaction rates of Amberlyst-15 are higher than the values recorded for the sulphonated composites (see Table 3) due to the high -$SO_3H$ density of Amberlyst-15 (see Table 2). TOF is here defined as (mmol product)·(mmol -$SO_3H$)$^{-1}$·(h)$^{-1}$ and it is used to compare catalytic performances in terms of intrinsic acid properties. A comparison of the TOF values of the different catalysts (Table 3) demonstrates that the sulphonated composites have considerably larger TOF values than those achieved with Amberlyst-15, indicating that they have a higher intrinsic catalytic activity. This may be due to the high hydrophilicity of sulphonated composites which facilitates the adsorption of a large amount of hydrophilic molecules such as ethanol and to the ready access of the reactants to the -$SO_3H$ sites which are located in easily approachable mesopores [45,46]. In the case of the esterification of maleic anhydride, the selectivity of this reaction is very important since, besides DEM, an undesirable trans-isomer product (diethyl fumarate, DEF) may also be formed. In this case, the sulphonated composites exhibited a better selectivity than Amberlyst-15. In order to evaluate the reusability of these acid catalysts, we examined the stability of a CSK-500 composite during the esterification of maleic anhydride over 4 cycles. The results presented in Figure 8 show that DEM yields remained almost constant after four cycles, which confirms its reusability as catalyst.

## 4. Conclusions

In summary, we have presented a novel synthesis procedure for the fabrication of solid acid catalysts consisting of a -$SO_3H$ functionalized carbon layer uniformly coating the pores of three mesoporous silica materials. The success of this strategy is based on the use of silica substrates with highly concentrated groups of silanol which can react via condensation reactions with the carbon precursor molecules (*i.e.* 2,3-dihydroxynaphthalene), thereby producing a layer of carbon that is uniformly distributed inside the silica pores. The resulting sulphonated silica-carbon composites have a high BET surface area (ever 590 $m^2 \cdot g^{-1}$), a large pore volume (1-1.8 $cm^3 \cdot g^{-1}$) and a porosity made up of uniform mesopores with a width of ~ 10 nm to ~ 29 nm. In addition, these sulphonated materials are characterised by a high density of acidic groups (-$SO_3H$, -COOH, and -OH) attached to the deposited carbon layer. The combination of the textural and chemical properties of these materials gives rise highly effective solid acids with a large number of strong acid sites (*i.e.* -$SO_3H$) located inside wide and accessible mesopores. This ensures high mass transfer rates. These solid acids were investigated as catalysts for the esterification of maleic anhydride, succinic acid and oleic acid with ethanol. The results obtained show that these materials have a high intrinsic catalytic activity (TOF), which is superior to that of commercial solid acids such as Amberlyst-15. The reusability of these sulphonated composites has been conformed in the case of the esterification of maleic anhydride with ethanol. The synthesis procedure reported in this study provides a new family of mesoporous silica-carbon materials that, due to their special properties, can be used not only as solid acid catalysts but also as catalytic supports and adsorbents for the immobilization of biomolecules and removal of heavy metals, by selecting the appropriate functional groups for the carbon layer.

**Acknowledgments**. This work was supported by Spanish MICINN (Project CQT2011-24776). M.S. and P.V-V. acknowledge the *Ramon y Cajal* and *JAE-Predoc* contracts respectively.

## References

[1] A. Sivasamy, K. Cheah, P. Fornasiero, F. Kemausuor, S. Zinoviev, and S. Miertus, Catalytic Applications in the Production of Biodiesel from Vegetable Oils, ChemSusChem 2 (2009) 278-300.

[2] P. T. Anastas and M. M. Kirchhoff, Origins, Current Status, and Future Challenges of Green Chemistry, Acc. Chem. Res. 35 (2002) 686-694.

[3] J. H. Clark, Solid Acids for Green Chemistry, Acc. Chem. Res. 35 (2002) 791-797.

[4] P. T. Anastas and J. B. Zimmerman, Peer Reviewed: Design Through the 12 Principles of Green Engineering, Environ. Sci. Technol. 37 (2003) 94A-101A.

[5] T. Okuhara, Water-Tolerant Solid Acid Catalysts, Chem. Rev. 102 (2002) 3641-3666.

[6] J. A. Melero, J. Iglesias, and G. Morales, Heterogeneous acid catalysts for biodiesel production: current status and future challenges, Green Chem. 11 (2009) 1285-1308.

[7] A. Corma and A. Martinez, Zeolites and Zeotypes as catalysts, Adv. Mater. 7 (1995) 137-144.

[8] M. A. Harmer and Q. Sun, Solid acid catalysis using ion-exchange resins, Appl. Catal. A: Gen. 221 (2001) 45-62.

[9] M. A. Harmer, Q. Sun, A. J. Vega, W. E. Farneth, A. Heidekum, and W. F. Hoelderich, Nafion resin-silica nanocomposite solid acid catalysts.Microstructure-processing-property correlations, Green Chem. 2 (2000).

[10] A. A. Kiss, A. C. Dimian, and G. Rothenberg, Solid Acid Catalysts for Biodiesel Production: Towards Sustainable Energy, Adv. Synth. Catal. 348 (2006) 75-81.

[11] V. L. Budarin, J. H. Clark, R. Luque, and D. J. Macquarrie, Versatile mesoporous carbonaceous materials for acid catalysis, Chem. Comm. (2007).

[12] S. Suganuma, K. Nakajima, M. Kitano, D. Yamaguchi, H. Kato, S. Hayashi, and M. Hara, Hydrolysis of cellulose by amorphous carbon bearing SO3H, COOH, and OH groups, J. Am. Chem. Soc. 130 (2008) 12787-12793.

[13] S. Suganuma, K. Nakajima, M. Kitano, H. Kato, A. Tamura, H. Kondo, S. Yanagawa, S. Hayashi, and M. Hara, SO3H-bearing mesoporous carbon with highly selective catalysis, Microp. Mesop. Mat. 143 (2011) 443-450.

[14] D. Zhao, J. Feng, Q. Huo, N. Melosh, G. H. Fredrickson, B. F. Chmelka, and G. D. Stucky, Triblock Copolymer Syntheses of Mesoporous Silica with Periodic 50 to 300 Angstrom Pores, Science 279 (1998) 548-552.

[15] D. Margolese, J. A. Melero, S. C. Christiansen, B. F. Chmelka, and G. D. Stucky, Direct Syntheses of Ordered SBA-15 Mesoporous Silica Containing Sulfonic Acid Groups, Chem. Mater. 12 (2000) 2448-2459.

[16] D. Das, J. F. Lee, and S. Cheng, Sulfonic acid functionalized mesoporous MCM-41 silica as a convenient catalyst for Bisphenol-A synthesis, Chem. Comm. (2001) 2178-2179.

[17] J. A. Melero, R. van Grieken, and G. Morales, Advances in the Synthesis and Catalytic Applications of Organosulfonic-Functionalized Mesostructured Materials, Chem. Rev. 106 (2006) 3790-3812.

[18] R. Xing, Y. Liu, Y. Wang, L. Chen, H. Wu, Y. Jiang, M. He, and P. Wu, Active solid acid catalysts prepared by sulfonation of carbonization-controlled mesoporous carbon materials, Microp. Mesop. Mat. 105 (2007) 41-48.

[19] X. Wang, R. Liu, M. M. Waje, Z. Chen, Y. Yan, K. N. Bozhilov, and P. Feng, Sulfonated Ordered Mesoporous Carbon as a Stable and Highly Active Protonic Acid Catalyst, Chem. Mater. 19 (2007) 2395-2397.

[20] R. Liu, X. Wang, X. Zhao, and P. Feng, Sulfonated ordered mesoporous carbon for catalytic preparation of biodiesel, Carbon 46 (2008) 1664-1669.

[21] L. Peng, A. Philippaerts, X. Ke, J. Van Noyen, F. De Clippel, G. Van Tendeloo, P. A. Jacobs, and B. F. Sels, Preparation of sulfonated ordered mesoporous carbon and its use for the esterification of fatty acids, Catal. Today 150 (2010) 140-146.

[22] P. Lin, B. Li, J. Li, H. Wang, X. Bian, and X. Wang, Synthesis of Sulfonated Carbon Nanocage and Its Performance as Solid Acid Catalyst, Cat. Lett. 141 (2011) 459-466.

[23] R. Liu, Y. Shi, Y. Wan, Y. Meng, F. Zhang, D. Gu, Z. Chen, B. Tu, and D. Zhao, Triconstituent Co-assembly to Ordered Mesostructured Polymer–Silica and Carbon–Silica Nanocomposites and Large-Pore Mesoporous Carbons with High Surface Areas, J. Am. Chem. Soc. 128 (2006) 11652-11662.

[24] Y. Zhang, F. L.-Y. Lam, X. Hu, and Z. Yan, Formation of an ink-bottle-like pore structure in SBA-15 by MOCVD, Chem. Comm. (2008) 5131-5133.

[25] H. Nishihara, Y. Fukura, K. Inde, K. Tsuji, M. Takeuchi, and T. Kyotani, Carbon-coated mesoporous silica with hydrophobicity and electrical conductivity, Carbon 46 (2008) 48-53.

[26] P. Valle-Vigón, M. Sevilla, and A. B. Fuertes, Mesostructured silica-carbon composites synthesized by employing surfactants as carbon source, Microp. Mesop. Mat. 134 (2010) 165-174.

[27] P. Gupta and S. Paul, Amorphous carbon-silica composites bearing sulfonic acid as solid acid catalysts for the chemoselective protection of aldehydes as 1,1-diacetates and for N-, O- and S-acylations, Green Chem. 13 (2011) 2365-2372.

[28] K. Nakajima, M. Okamura, J. N. Kondo, K. Domen, T. Tatsumi, S. Hayashi, and M. Hara, Amorphous Carbon Bearing Sulfonic Acid Groups in Mesoporous Silica as a Selective Catalyst, Chem. Mater. 21 (2008) 186-193.

[29] L. FANG, K. ZHANG, X. LI, H. Wu, and P. Wu, Preparation of a Carbon-Silica Mesoporous Composite Functionalized with Sulfonic Acid Groups and Its Application to the Production of Biodiesel, Chinese Journal of Catalysis 33 (2012) 114-122.

[30] Y. Liu, J. Chen, J. Yao, Y. Lu, L. Zhang, and X. Liu, Preparation and properties of sulfonated carbon-silica composites from sucrose dispersed on MCM-48, Chem. Eng. J. 148 (2009) 201-206.

[31] D. Zhao, Q. Huo, J. Feng, B. F. Chmelka, and G. D. Stucky, Nonionic Triblock and Star Diblock Copolymer and Oligomeric Surfactant Syntheses of Highly Ordered, Hydrothermally Stable, Mesoporous Silica Structures, J. Am. Chem. Soc. 120 (1998) 6024-6036.

[32] F. Kleitz, S. H. Choi, and R. Ryoo, Cubic Ia3d large mesoporous silica: synthesis and replication to platinum nanowires, carbon nanorods and carbon nanotubes, Chem. Comm. (2003) 2136-2137.

[33] P. Schmidt-Winkel, W. Wayne, D. Zhao, P. Yang, B. F. Chmelka, and G. D. Stucky, Mesocellular Siliceous Foams with Uniformly Sized Cells and Windows, J. Am. Chem. Soc. 121 (1998) 254-255.

[34] P. F. Fulvio, S. Picus, and M. Jaroniec, SBA-15-Supported Mixed-Metal Oxides: Partial Hydrolytic Sol-Gel Synthesis, Adsorption, and Structural Properties, ACS Appl. Mater. Interfaces 2 (2009) 134-142.

[35] M. Kruk, M. Jaroniec, and A. Sayari, Application of large pore MCM-41 molecular sieves to improve pore size analysis using nitrogen adsorption measurements, Langmuir 13 (1997) 6267-6273.

[36] X. Mo, D. E. López, K. Suwannakarn, Y. Liu, E. Lotero, J. Goodwin, and C. Lu, Activation and deactivation characteristics of sulfonated carbon catalysts, J. Catal. 254 (2008) 332-338.

[37] J. Janaun and N. Ellis, Role of silica template in the preparation of sulfonated mesoporous carbon catalysts, Appl. Catal. A: Gen. 394 (2011) 25-31.

[38] M. Okamura, A. Takagaki, M. Toda, J. N. Kondo, K. Domen, T. Tatsumi, M. Hara, and S. Hayashi, Acid-catalyzed reactions on flexible polycyclic aromatic carbon in amorphous carbon, Chem. Mater. 18 (2006) 3039-3045.

[39] R. S. McDonald, Surface Functionality of Amorphous Silica by Infrared Spectroscopy, J. Phys. Chem. 62 (1958) 1168-1178.

[40] B. A. Morrow and A. J. McFarlan, Infrared and gravimetric study of an aerosil and a precipitated silica using chemical and H/D exchange probes, Langmuir 7 (1991) 1695-1701.

[41] A. Zecchina, S. Bordiga, G. Spoto, L. Marchese, G. Petrini, G. Leofanti, and M. Padovan, Silicalite characterization. 2. IR spectroscopy of the interaction of carbon monoxide with internal and external hydroxyl groups, The Journal of Physical Chemistry 96 (1992) 4991-4997.

[42] P. Valle-Vigón, M. Sevilla, and A. B. Fuertes, Synthesis of Uniform Mesoporous Carbon Capsules by Carbonization of Organosilica Nanospheres, Chem. Mater. 22 (2010) 2526-2533.

[43] T. Jawhari, A. Roid, and J. Casado, Raman spectroscopic characterization of some commercially available carbon black materials, Carbon 33 (1995) 1561-1565.

[44] G. Socrates, Infrared and Raman Characteristic Group Frequencies, Wiley, New York 2005.

[45] A. Takagaki, M. Toda, M. Okamura, J. N. Kondo, S. Hayashi, K. Domen, and M. Hara, Esterification of higher fatty acids by a novel strong solid acid, Catal. Today 116 (2006) 157-161.

[46] K. Nakajima, M. Hara, and S. Hayashi, Environmentally Benign Production of Chemicals and Energy Using a Carbon-Based Strong Solid Acid, J. Am. Ceram. Soc. 90 (2007) 3725-3734.

**Table 1.** Structural properties of the silica samples, and silica-carbon composites and sulphonated silica-carbon composites

| Silica Template | Sample | Carboneous matter (wt %) | $S_{BET}$ ($m^2.g^{-1}$) | $V_p$ ($cm^3.g^{-1}$) [a] | Pore size (nm) [b] |
|---|---|---|---|---|---|
| KIT-6 | K | - | 560 | 1.28 | 10.1 |
| | CK-500 | 28.5 | 540 | 0.81 | 8.6 |
| | CSK-500 | 34 | 590 | 1.00 | 10.2 |
| SBA-15 | S | - | 510 | 1.1 | 10.4 |
| | CS-500 | 28.7 | 490 | 0.73 | 8.7 |
| | CSS-500 | 26.8 | 530 | 0.91 | 10.5 |
| | C(S) | 100 | 1080 | 1.05 | 3.9 |
| Mesocellular silica | MS | - | 570 | 2.21 | 30 |
| | CMS-500 | 33 | 520 | 1.71 | 28 |
| | CSMS-500 | 33 | 520 | 1.8 | 28.8 |

[a] As deduced by TGA analyses; [b] Pore volume determined at $p/p_o=0.99$;
[c] Maximum of pore size distribution.

**Table 2**: Acid density of the sulphonated silica-carbon composites.

| Catalyst | Acid density ($mmol \cdot g^{-1}$) | | | |
|---|---|---|---|---|
| | Total [a] | $-SO_3H$ [b] | -COOH [c] | -OH [d] |
| Amberlyst 15 | 5.1 | 4.7 | - | - |
| CSS-500 | 2.9 | 0.39 | 0.87 | 1.63 |
| CSK-500 | 3.0 | 0.38 | 0.85 | 1.80 |
| CSMS-500 | 3.9 | 0.35 | 1.19 | 2.36 |

[a] Calculated by titration with NaOH (0.05 N); [b] Obtained by elemental analysis; [c] Calculated by titration with $NaHCO_3$ (0.05 N) and subtracting the $-SO_3H$ content; [d] Estimated from the difference between the total, $-SO_3H$ and -COOH acid densities.

**Table 3**. Catalytic activity of Amberlyst-15 and the sulphonated silica-carbon composites treated at 500 ºC in the esterification reactions.

| Catalyst | Maleic anhydride esterification | | | Succinic acid esterification | | Oleic acid esterification | |
|---|---|---|---|---|---|---|---|
| | Initial rate [a] ($\mu mol \cdot g^{-1} \cdot s^{-1}$) | TOF [b] ($h^{-1}$) | S (%) [c] | Initial rate [a] ($\mu mol \cdot g^{-1} \cdot s^{-1}$) | TOF [b] ($h^{-1}$) | Initial rate [a] ($\mu mol \cdot g^{-1} \cdot s^{-1}$) | TOF [b] ($h^{-1}$) |
| Amberlyst 15 | 6.5 | 5 | 93 | 1.2 | 0.9 | 7.4 | 5.6 |
| CSS-500 | 2.5 | 38 | >95 | 0.7 | 6.4 | 3.3 | 31 |
| CSK-500 | 3.7 | 34 | 95 | 0.5 | 4.8 | 2.8 | 26 |
| CSMS-500 | 3.4 | 35 | >95 | 0.5 | 5.1 | 3.1 | 31 |

[a] Initial rate of reaction, defined as the amount of product formed per unit of time and mass of catalyst.
[b] TOF = Turnover frequency, defined as mmol product per mmol of active site ($-SO_3H$) and time.
[c] S = Selectivity defined as DEM/(DEM+DEF) x 100

# LEGENDS

**Scheme 1.** Illustration of the method used to prepare mesostructured sulphonated silica-carbon composites. (A) Surfactant-silica, (B) Free surfactant silica, (C) DN-silica hybrid, (D) silica-carbon composite and (E) sulphonated silica-carbon composite.

**Figure 1.** SEM micrographs of: SBA-15 (A), CS-500 (B), CSS-500 (C), KIT-6 (D), CK-500 (E), CSK-500 (F), MS (G), CMS-500 (H) and CSMS-500 (I).

**Figure 2.** Nitrogen sorption isotherms and pore size distributions (insets) of the silica, silica-carbon composites, and sulphonated silica-carbon composites: (a) SBA-15, CS-500 and CSS-500; (b) KIT-6, CK-500 and CSK-500; (c) MS, CMS-500 and CSMS-500**.**

**Figure 3.** TEM images of: (A) CS-500, (B) CSS-500, (C) CK-500, (D) CSK-500, (E) CMS-500 and (F) CSMS-500.

**Figure 4.** FTIR spectra for SBA-15, the corresponding composite (CS-500) and the three sulphonated silica-carbon composites carbonized at 500 ºC (CSS-500, CSK-500 and CSMS-500).

**Figure 5.** (a) S 2p core level XPS spectrum of the CSK-500 composite after removal of the silica with HF. (b) Raman spectra for the three sulphonated silica-carbon samples.

**Figure 6**. Concentration of the evolved gases during the CSS-500 TPD experiment. (Under argon and a heating rate of 5 $^{o}C \cdot min^{-1}$).

**Figure 7**. Illustration of the esterification reactions and the product formation profiles with time for: a) Maleic anhydride, b) Succinic acid and c) Oleic acid esterifications.

**Figure 8**. Reusability of the CSK-500 catalyst in the esterification of maleic anhydride with ethanol.

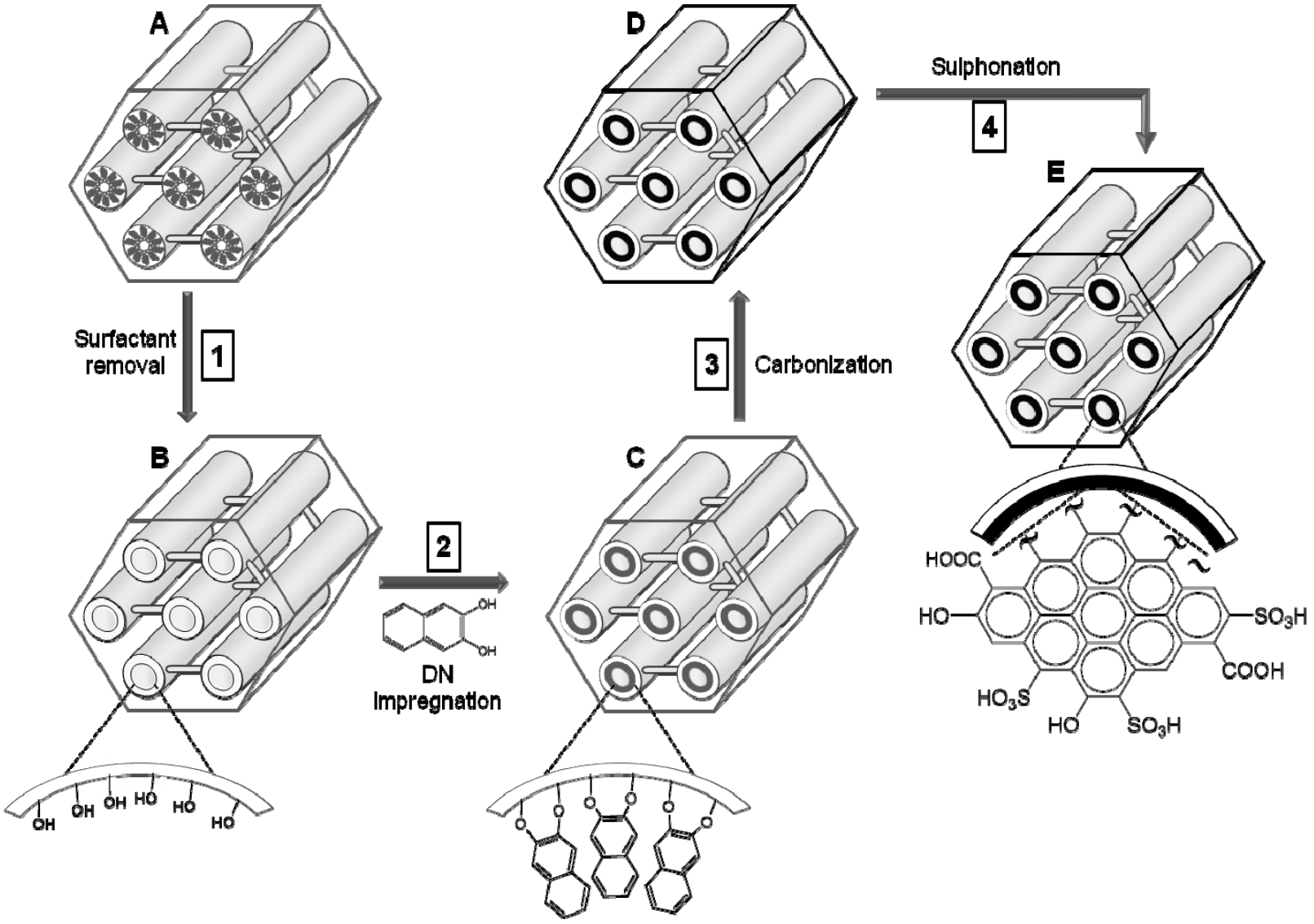
A
Surfactant removal
1
B
2
DN Impregnation
C
3
Carbonization
D
Sulphonation
4
E
OH
OH
OH
HO
HO
HO
HOOC
HO
SO3H
COOH
HO3S
HO
SO3H

Scheme 1

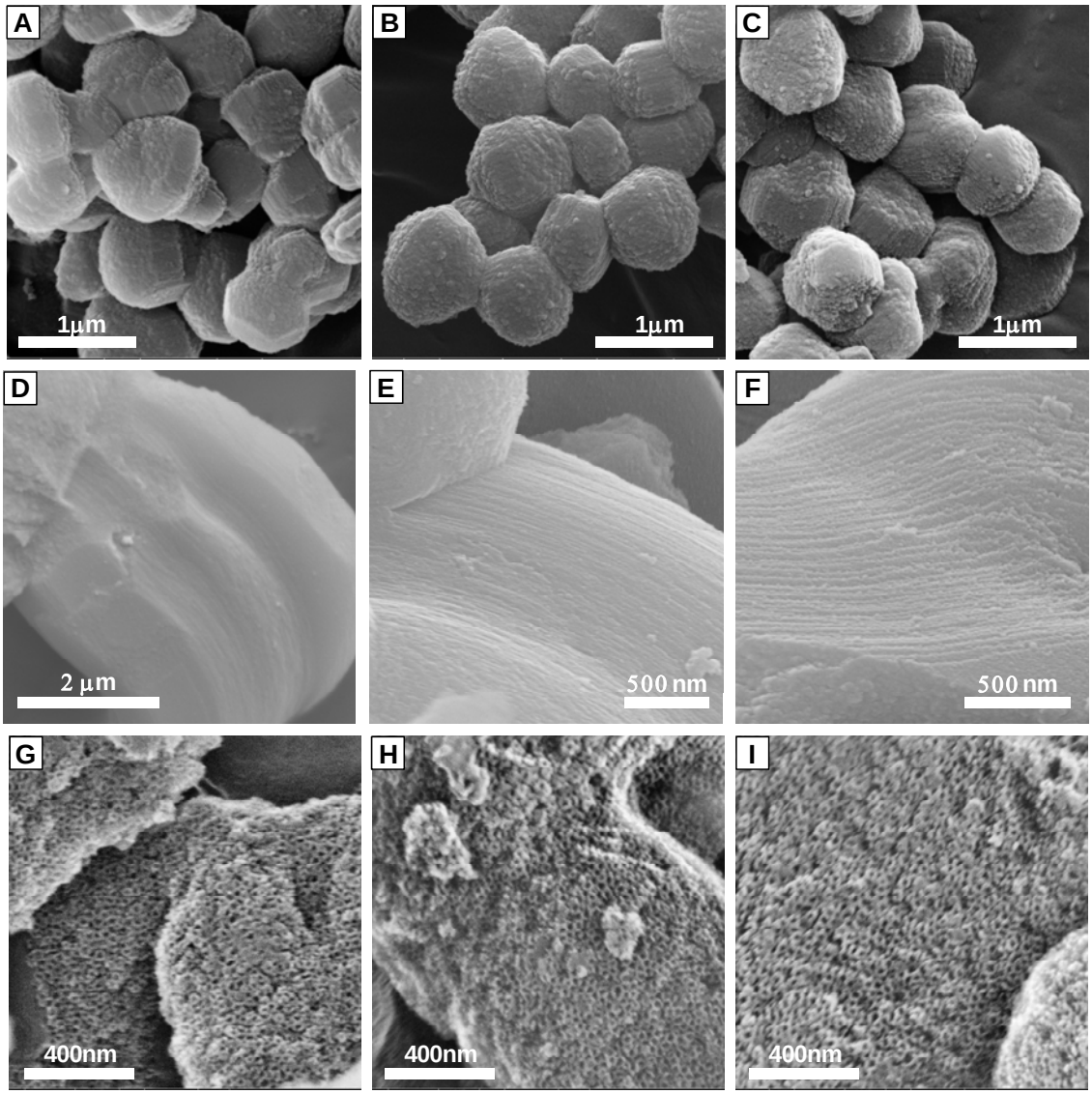


Figure 1

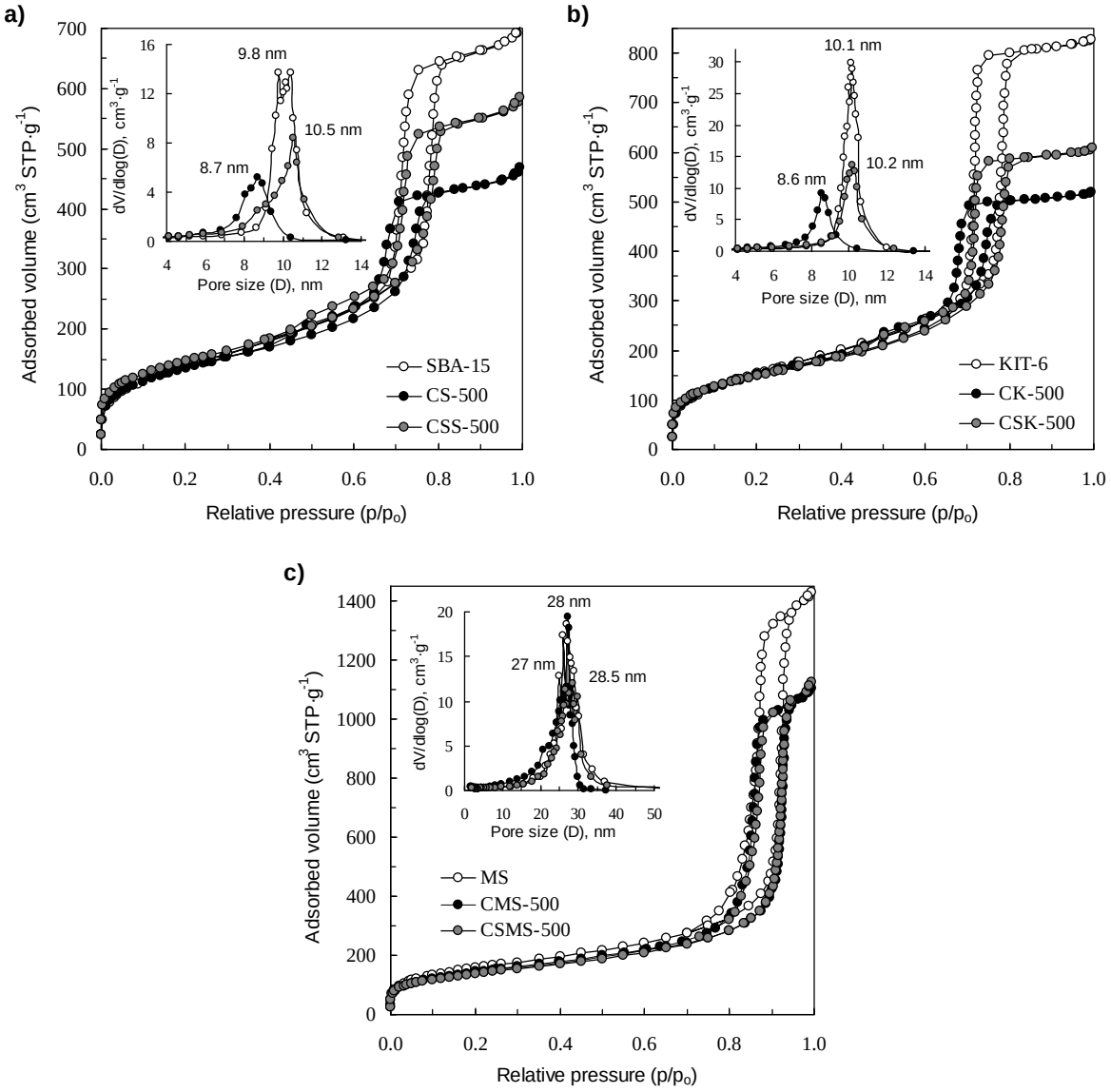
a)
Adsorbed volume (cm3 STP·g-1)
Relative pressure (p/po)
dV/dlog(D), cm3·g-1
Pore size (D), nm
9.8 nm
10.5 nm
8.7 nm
SBA-15
CS-500
CSS-500
b)
Adsorbed volume (cm3 STP·g-1)
Relative pressure (p/po)
dV/dlog(D), cm3·g-1
Pore size (D), nm
10.1 nm
10.2 nm
8.6 nm
KIT-6
CK-500
CSK-500
c)
Adsorbed volume (cm3 STP·g-1)
Relative pressure (p/po)
dV/dlog(D), cm3·g-1
Pore size (D), nm
28 nm
27 nm
28.5 nm
MS
CMS-500
CSMS-500

Figure 2

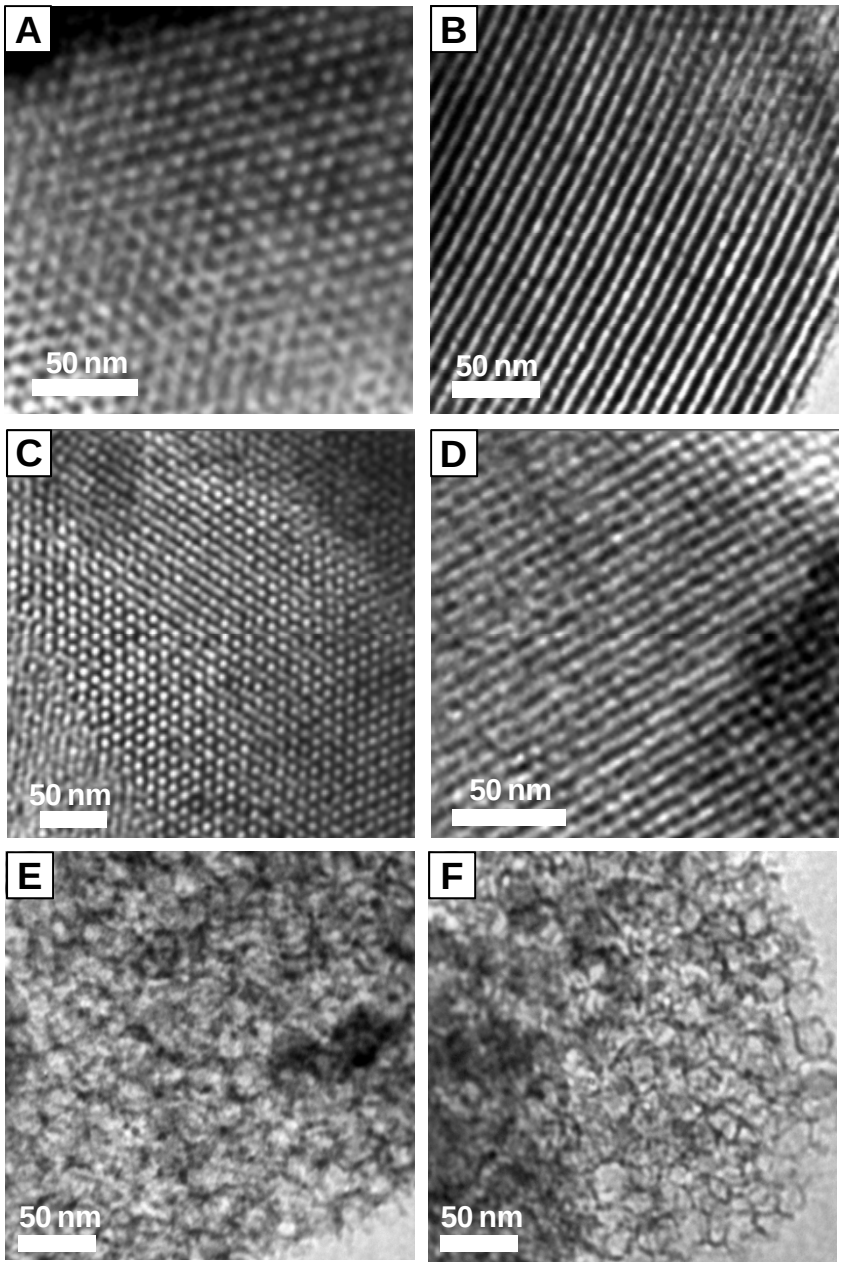


Figure 3

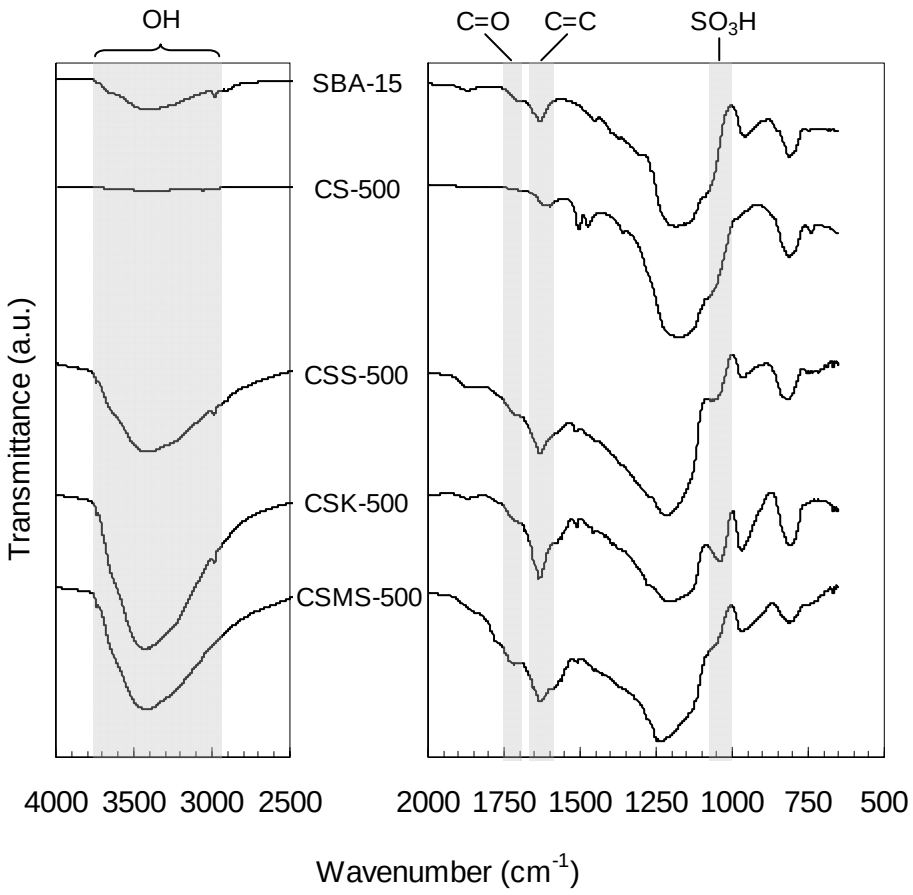


Figure 4

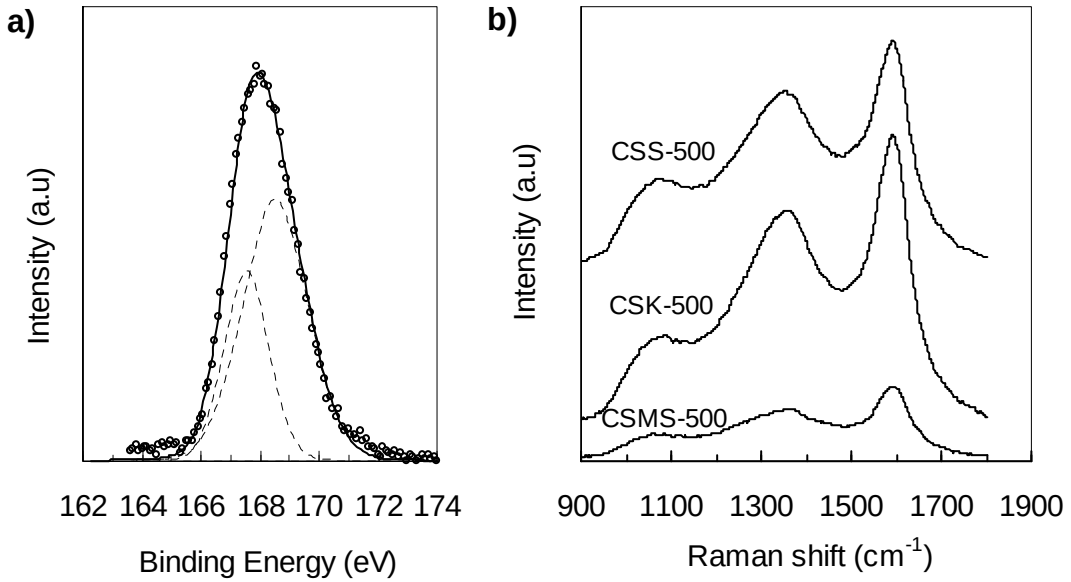


Figure 5

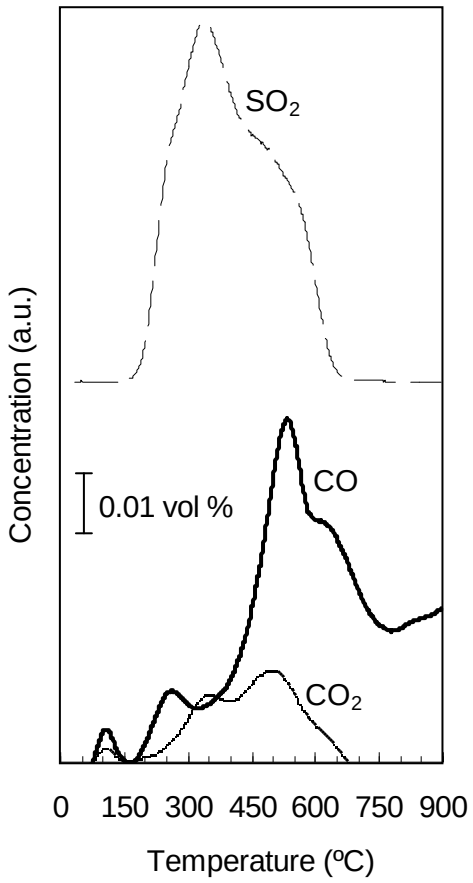
SO2
Concentration (a.u.)
0.01 vol %
CO
CO2
0 150 300 450 600 750 900
Temperature (ºC)

Figure 6

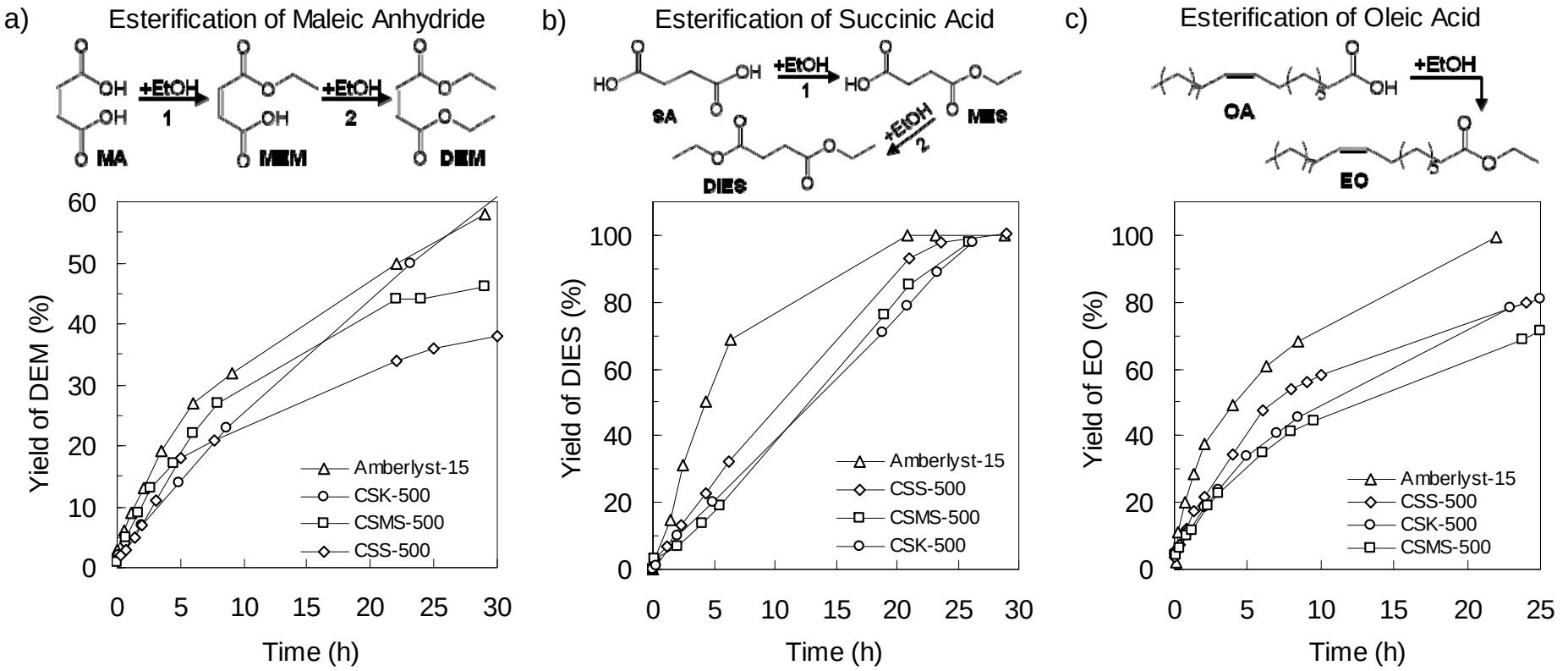
a)
Esterification of Maleic Anhydride
+EtOH
1
+EtOH
2
MA
MEM
DEM
Yield of DEM (%)
Time (h)
Amberlyst-15
CSK-500
CSMS-500
CSS-500
b)
Esterification of Succinic Acid
SA
MES
DIES
Yield of DIES (%)
Time (h)
Amberlyst-15
CSS-500
CSMS-500
CSK-500
c)
Esterification of Oleic Acid
OA
EO
Yield of EO (%)
Time (h)
Amberlyst-15
CSS-500
CSK-500
CSMS-500

Figure 7

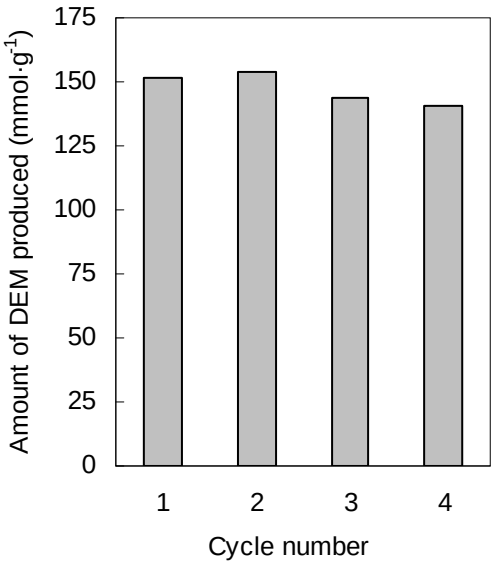
175
150
125
100
75
50
25
0
Amount of DEM produced (mmol·g-1)
1
2
3
4
Cycle number

Figure 8